

Research article

Open Access

Comparative 3-D Modeling of tmRNA

Jody Burks¹, Christian Zwieb*², Florian Müller³, Iwona Wower¹ and Jacek Wower¹

Address: ¹Department of Animal Sciences, Cellular and Molecular Biosciences Program, Auburn University, Auburn, AL 36849 USA, ²Department of Molecular Biology, University of Texas Health Science Center at Tyler, 11937 US Hwy 271, Tyler, 75708 TX USA and ³Max Planck Institute for Molecular Genetics, Ihnestrasse 73, D-14195, Berlin, Germany

Email: Jody Burks - burksjm@auburn.edu; Christian Zwieb* - zwieb@uthct.edu; Florian Müller - pentafolium-soft@web.de; Iwona Wower - iwower@acesag.auburn.edu; Jacek Wower - jwower@acesag.auburn.edu

* Corresponding author

Published: 15 June 2005

Received: 28 January 2005

BMC Molecular Biology 2005, 6:14 doi:10.1186/1471-2199-6-14

Accepted: 15 June 2005

This article is available from: <http://www.biomedcentral.com/1471-2199/6/14>

© 2005 Burks et al; licensee BioMed Central Ltd.

This is an Open Access article distributed under the terms of the Creative Commons Attribution License (<http://creativecommons.org/licenses/by/2.0>), which permits unrestricted use, distribution, and reproduction in any medium, provided the original work is properly cited.

Abstract

Background: *Trans*-translation releases stalled ribosomes from truncated mRNAs and tags defective proteins for proteolytic degradation using transfer-messenger RNA (tmRNA). This small stable RNA represents a hybrid of tRNA- and mRNA-like domains connected by a variable number of pseudoknots. Comparative sequence analysis of tmRNAs found in bacteria, plastids, and mitochondria provides considerable insights into their secondary structures. Progress toward understanding the molecular mechanism of template switching, which constitutes an essential step in *trans*-translation, is hampered by our limited knowledge about the three-dimensional folding of tmRNA.

Results: To facilitate experimental testing of the molecular intricacies of *trans*-translation, which often require appropriately modified tmRNA derivatives, we developed a procedure for building three-dimensional models of tmRNA. Using comparative sequence analysis, phylogenetically-supported 2-D structures were obtained to serve as input for the program ERNA-3D. Motifs containing loops and turns were extracted from the known structures of other RNAs and used to improve the tmRNA models. Biologically feasible 3-D models for the entire tmRNA molecule could be obtained. The models were characterized by a functionally significant close proximity between the tRNA-like domain and the resume codon. Potential conformational changes which might lead to a more open structure of tmRNA upon binding to the ribosome are discussed. The method, described in detail for the tmRNAs of *Escherichia coli*, *Bacillus anthracis*, and *Caulobacter crescentus*, is applicable to every tmRNA.

Conclusion: Improved molecular models of biological significance were obtained. These models will guide in the design of experiments and provide a better understanding of *trans*-translation. The comparative procedure described here for tmRNA is easily adopted for the modeling the members of other RNA families.

Background

Transfer-messenger RNA (tmRNA), also known as 10Sa RNA or *ssrA* RNA, is a hybrid of a tRNA-like domain (TLD) and a mRNA-like domain (MLD) connected by a variable number of pseudoknots [1]. TmRNA is a stable and essential component of *trans*-translation, a quality-control process that rescues ribosomes stalled on mRNAs lacking stop codons. During *trans*-translation, ribosomes switch from a defective mRNA (lacking its translation-termination signal) to the MLD of tmRNA. Because a stop codon is provided by the tmRNA, the ribosomes can dissociate and recycle [2]. As an additional advantage, the tandem translation of the two templates generates a tagged polypeptide which is degraded by housekeeping proteases [3,4].

For tagging, tmRNA has to be charged by aminoacyl-tRNA synthetases [5]. Assisted by protein SmpB, the charged tmRNA is delivered to stalled ribosomes as a quaternary complex with EF-Tu and GTP. Binding of tmRNA to ribosomes is facilitated by ribosomal protein S1, which interacts with the MLD and pseudoknots but not with the TLD [6-9]. Recently, cryo-EM revealed the shape of the tmRNA associated with SmpB and EF-Tu in its ribosome-bound form [10]. Despite this significant progress, high-resolution structures as obtained by NMR and X-ray crystallography are unavailable and expected to be difficult to obtain in the foreseeable future due to the relatively large size and flexibility of the tmRNA.

In the present work we used a stepwise procedure for arriving at high-resolution models for the entire tmRNA molecule. First, 2-D structures were obtained by covariation analysis of a large number of tmRNA sequences. The basepairing information was submitted to the ERNA-3D modeling program [11] to build the helical sections. Structural motifs of the loops and turns were identified in SCOR [12], high-resolution data were extracted from known structures, and these data were incorporated into the models. Overall, significantly improved 3-D models were obtained which will be useful to understand the role of tmRNA in *trans*-translation. The described approach can be adapted to obtain high-resolution models of the members of other RNA families.

Results

Identification of tmRNA sequences

The tmRNA sequences were identified previously and subjected to comparative sequence analysis (CSA) as described [1,13]. New tmRNA sequences were obtained from the tmRNA website [14], through keyword searches of the literature and GenBank [15], or BLAST [16,17], and various genome sequencing projects. The new sequences were examined iteratively as described in Materials and

Methods to confirm tmRNA identity, remove sequence duplications, and create a meaningful alignment.

New potential tmRNA sequences were maintained as a preliminary alignment in BioEdit [18], separate EMBL-formatted sequence files, and a HTML-formatted phylogenetic list. The sequences were ordered phylogenetically using the information in the Ribosomal Database Project (RDP) [19]. If the organism name was not listed in the RDP, the sequence was placed next to its closest relative using the NCBI Taxonomy resource [20].

Selection of tmRNA sequences

The new sequences were confirmed individually as tmRNAs by comparison with the closest relative using the pairwise alignment feature of BioEdit [18]. If there was a lack of obvious similarity, the sequence was inspected for evidence of biological features such as the ability to form a TLD and an open reading frame. Furthermore, the possibility of a two-part tmRNA was considered. A sequence suspected to be a new tmRNA was investigated further by CSA [13] as described in Materials and Methods.

Potential new sequences of the alpha-Proteobacteria and some Cyanobacteria that were encoded in two separate sections of their genes [21], were compared to the two-part tmRNA sequence from a closest relative for effective comparison with the one-part tmRNAs. The 3'- and 5'-ends of each section were determined by pairwise alignment to generate a single sequence. Each of the 20 new two-part tmRNAs (14 sequences from alpha-Proteobacteria and six from Cyanobacteria) was subjected to this rearrangement.

Comparative Sequence Analysis

Sequences were ordered phylogenetically using the RDP [19] as a guide or by alignment with the closest relative. Identical regions were aligned first. Subsequently, similar regions were aligned using invariant positions as signposts. Regions of biological significance, such as the resume and stop codons, were then considered. Finally, common secondary structure features were used to align regions that lacked primary structure similarity or biological features. Supported Watson-Crick basepairs and G-U interactions were indicated in the alignment by uppercase letters. Gaps were introduced to account for differences in sequence length and to avoid the alignment of dissimilar regions.

Secondary structure was determined using covariation analysis as described [13] (see also Materials and Methods). The alignment was examined to identify compensatory base changes (CBCs) and other covariations. The numbers of CBCs and mismatches between the alignment columns were counted. CBCs provided positive evidence

Table 1: Phylogenetic distribution of tmRNA features

Phylogenetic Group	TLD	MLD	pk1	pk2	pk3	pk4	Other
Thermophilic Oxygen Reducers							
Thermatogales							
Green Non-sulfur & Bacteria relatives							
Flexibacter Cytophaga Bacteroides							
Green Sulfur Bacteria							
Planctomyces & relatives							
Cyanobacteria					1	1,2	3
Plastids					-	-	
Mitochondria		-	-	-	-	-	
Fibrobacter/Acidobacter & relatives							
Spirochetes & relatives							
Proteobacteria, alpha				4		5	3
Proteobacteria, beta				6			3
Proteobacteria, gamma				6			
Proteobacteria, delta							
Proteobacteria, epsilon							
Fusobacteria							
Gram Positive Bacteria							

The tRNA-like domain (TLD), mRNA-like domain (MLD), and the four pseudoknots pk1 to pk4 are shown on the top. Other features peculiar to a phylogenetic group are in the right column. White fields indicate the presence, dashes the absence of a feature. Numbers suggest the following structural features: (1) certain Cyanobacteria lack these pseudoknots. (2) One-chain cyanobacterial tmRNAs contain two smaller tandem pseudoknots named pk4a and 4b. (3) The tmRNAs of some species in this group consist of two basepaired molecules [14, 21]. (4) The genus *Rickettsia* and its relatives lack pk2. (5) pk4 of the alpha-Proteobacteria has been reduced to a single helix (named helix 11). (6) Some species in this group contain an additional helix (helix 6d).

for the existence of a basepair; mismatches provided negative evidence. If the number of compensatory base changes was two times or greater than the number of mismatches, the basepair was considered supported. If a basepair was invariant, no evidence for or against its existence could be gained from CSA. A basepair was considered specific to a particular phylogenetic group if it was proven only in that group.

Quality control

To check for the proper assignment of basepairs, the alignment was sent through an automated pipeline of programs from RNAdbTools [22]. The output was inspected visually and corrections were made manually using the BioEdit program [18]. The revised alignment was resubmitted to RNAdbTools, and the review process was repeated until a satisfactory alignment was produced.

TmRNA alignment

The final alignment contained a total of 274 tmRNA sequences in 16 bacterial phylogenetic groups. A complete phylogenetic list is available at the tmRDB [23]. There was a substantial increase in the number of two-part tmRNAs for a total of 27 sequences: 20 from alpha-Proteobacteria (20 tmRNAs), one mitochondrial tmRNA, and six cyanobacterial tmRNAs. The nine organelle sequences included one from a cyanelle, six from chloroplasts, one

from a plastid, and one from the *Reclinomonas americana* mitochondrion. The typical tmRNA was about 350 nucleotides long. The *R. americana* mitochondrion tmRNA contained only 189 nucleotides and, since it appeared to lack an ORF, may not be functional. Excluding this exception and any partial tmRNAs, the tmRNA of *Synechococcus* species PCC7009 was the shortest (250 nucleotides), and the longest was from *Chlamydomophila psittaci* (425 nucleotides). The tmRNA alignment is provided as additional files 1: tmRNA-alignment.html, 2: tmRNA-alignment-wide.txt, 3:tmRNA-alignment-92col.txt, and 4: tmRNA-alignment.msf.

Secondary structure of tmRNA

The tmRNA secondary structure features were extracted from the alignment and are listed in phylogenetic order in Table 1. The representative secondary structure of *Escherichia coli* tmRNA is shown in Figure 1. Secondary structures of *Bacillus anthracis* and *Caulobacter crescentus* are presented in as additional file 5: Banthracis2D.pdf and additional file 6: Ccrescentus2D.pdf, respectively.

TLD (helices 1, 2a and 12)

Although a prominent feature of each tmRNA, the TLD was relatively weakly supported by CSA due to a high degree of sequence conservation. However, the structure

tmRNA (*Escherichia coli*)

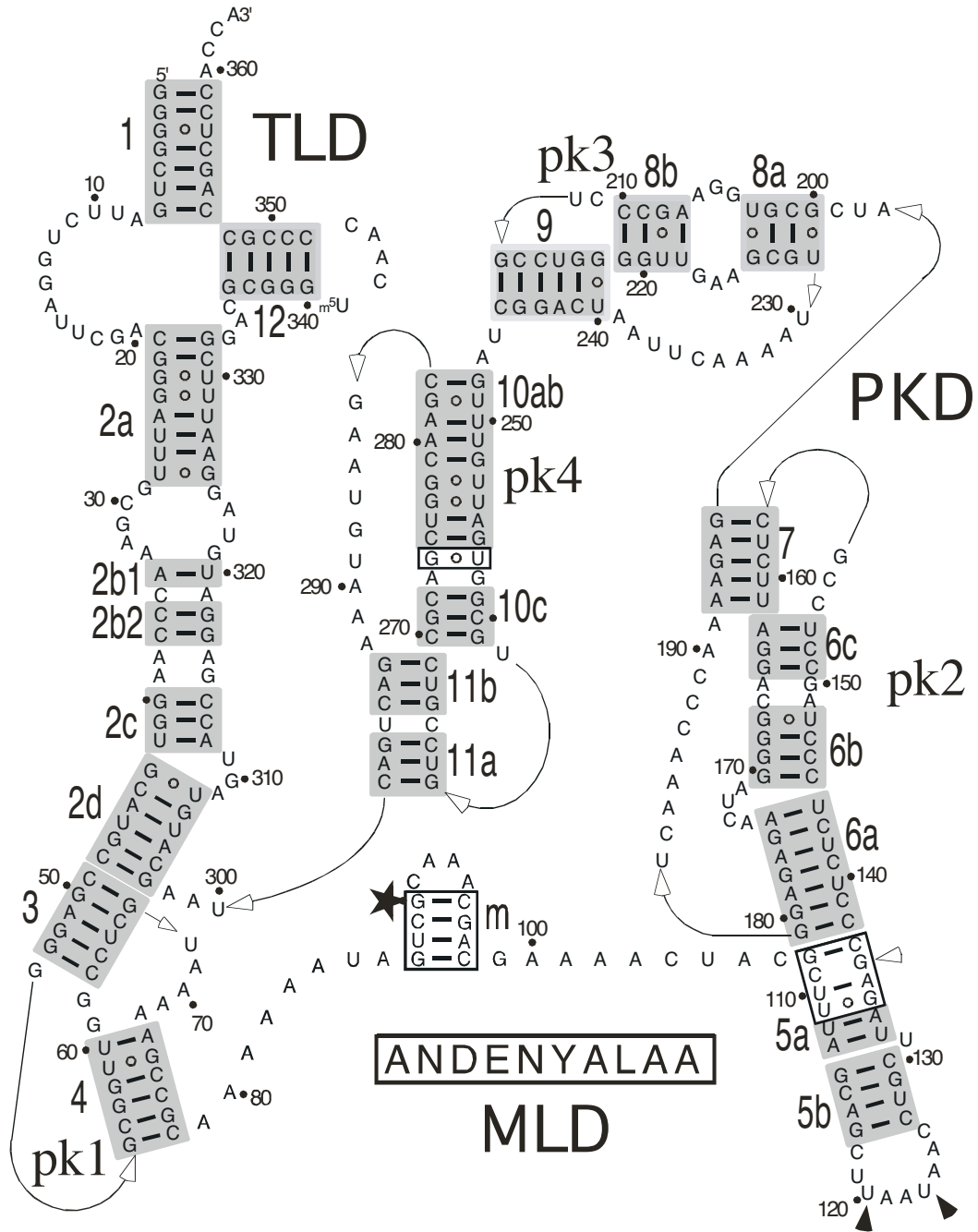


Figure 1

Secondary structure of *E. coli* tmRNA. Phylogenetically-supported helices are highlighted in gray and numbered from 1 to 12. The 5' and 3' ends are indicated. Arrows represent connections from 5' to 3'. Residues are numbered in increments of ten. Weakly supported regions and basepairs are shown in boxes. The disproved potential pairing of C109 with G136 is labeled with an open arrowhead. The star labels the first nucleotide of the resume codon. The tag peptide sequence is shown below the mRNA-like region. The stop codons are indicated with solid arrowheads. Three domains are distinguished: the tRNA-like domain (TLD), the mRNA-like domain (MLD), and the pseudoknot domain (PKD).

of this region is well established by experimental evidence [24-26].

Helix 1 contained seven basepairs and was usually continuous with the exception of the *Anabaena* species tmRNA, which contained an insertion in the 3'-portion of helix 1. The first pair (1G-C359 in *E. coli* tmRNA) was conserved with one exception in *Alcaligenes eutrophus* where there was a 1U-C345 mismatch possibly due to a sequencing error. The second (2G-C358, *E. coli* numbering, Figure 1) and third pair (3G-U357) of helix 1 were invariant and therefore neither supported nor disproved by CSA. The identities of the bases involved in the fourth (4G-C356) and fifth pair varied. The closing pair of helix 1 (7G-C353) was conserved with the exception of a 7U-A388 pair the *Trichodesmium erythraeum* tmRNA. The single-stranded region between helices 1 and 2a ranged from ten in *Dehalococcoides ethenogenes* to 13 nucleotides in one *Clostridium acetobutylicum* sequence. A U-A basepair (U6 in chain A with A88 in chain B) was possible in the *R. americana* mitochondrion tmRNA.

Helix 2a was equivalent to the anticodon stem of tRNA and contained eight supported basepairs as well as a short variable internal loop in the 5' half of the helix that occurred in a few sequences (e.g. *Caulobacter crescentus*, see additional file 6: Ccrescentus2D.pdf). The first position in the helix was a conserved cytosine (C21 in *E. coli*) which formed a weakly-supported basepair with the conserved G333. The partial tmRNA from the chloroplast of *Pavlova lutheri* contained a uracil in the first position, but no information regarding the 3' portion of helix 2a was available.

The T-loop and helix 12 were highly conserved, although many sequences lacked information about helix 12 due to primer annealing during PCR amplification. Helix 12 contained four strongly supported basepairs and a fifth conserved G-C pair (340G-C348 in *E. coli*; Figure 1). The *Dehalococcoides ethenogenes* tmRNA had the potential to form a sixth basepair in helix 12. Helix 12 was almost always continuous, except for the tmRNA of *Carboxydotherrmus hydrogenoformans* which possessed four basepairs and a mismatched U333 and C347. A 331-GG-332 preceded U333 in *C. hydrogenoformans* and followed the conserved 328-GAC-330. Therefore, U333 was unlikely to pair. In the T-loop, the U341 and U342 (*E. coli* tmRNA) seen in most sequences were replaced by two guanines in the tmRNA from the *R. americana* mitochondrion (G79 and G80 in chainB) [21]. In the tmRNA from *Caulobacter crescentus*, the nucleotide corresponding to U342 in *E. coli* tmRNA was changed to G62 in chainB (see additional file 6: Ccrescentus2D.pdf).

Helical sections 2b, 2c and 2d

Overall, sections 2b, 2c, and 2d were well supported. Sections 2a and 2b were separated by a variable loop ranging from one to seven nucleotides in the 5' portion and from one to nine nucleotides in the 3' portion. Sections 2b and 2c had the potential to form a continuously stacked helix (e.g. in *Chlamydomophila psittaci* tmRNA). Usually, a bulge of two to six nucleotides separated helical sections 2c and 2d (residues 309-311 in *E. coli* tmRNA, Figure 1). An asymmetrical loop was present in some sequences (for example, residues 40-41 in chainA, and 27-31 in chainB of *Caulobacter crescentus* tmRNA, see additional file 6: Ccrescentus2D.pdf). Helix 2d was the most conserved of the three helical sections. The G43-U308 basepair (*E. coli* numbering) in helix 2d was only weakly supported, conserved in most phylogenetic groups, but altered in the Thermatogales, Cyanobacteria, alpha-Proteobacteria, and Gram-positive bacteria. A 46A-U334 pair was possible in the *Synechocystis* species PCC6803 tmRNA.

Pseudoknot 1 (helices 3 and 4)

Pseudoknot 1 (pk1) was well supported. Of the three connecting regions, the two 5'-regions were very short (no or only one residue) while the third was relatively long (one to 11 residues). All pseudoknots in tmRNA followed the same general design [27]. Most sequences contained helices 3 and 4, with the exception of the tmRNA from *Oenococcus oeni* and the partial sequence from the chloroplast of *Pavlova lutheri*, both of which lacked helix 4 and thus did not form a pseudoknot. Helix 3 usually contained five basepairs. However, a sixth pair was possible in some bacteria.

Helix 4 could be split into helical sections 4a and 4b by a bulge seen in 46 sequences (position 57 in *B. anthracis* tmRNA; see additional file 5: Banthracis2D.pdf) or an internal loop seen in 52 tmRNA sequences. The adenine-rich terminal loop between the downstream halves of helices 3 and 4 ranged in length from two to 13 nucleotides.

The mRNA-like region (MLD)

The MLD consisted of an open reading frame (ORF) preceding helix 5 and varied from 48 (*Heliobacillus mobilis*) to 126 nucleotides (*Odontella sinensis* chloroplast). The resume codon usually coded for alanine, but for glycine in 30 sequences (e.g. *Bacillus anthracis*), aspartic acid in three sequences (e.g. *Staphylococcus epidermidis*), arginine in two uncultured species (FS1 and LEM2), serine in the uncultured species RCA1, and glutamic acid in *Mycoplasma pulmonis*.

Although helix 5 was only weakly supported by CBCs, recent site-directed mutagenesis experiments combined with functional studies *in vivo* and *in vitro* [28] provide strong evidence for its existence. One to three stop codons

were located within the helix 5 loop. A single UAA stop codon was present in 157 sequences. UAG (17 sequences) or UGA (10 sequences) were used less frequently. In 85 sequences there were two in-frame stop codons, where UAA was always the first codon, followed by another UAA (73 sequences), UAG (10 sequences) or UGA (2 sequences). Curiously, two sequences (*Bacillus megaterium* and *Chloroflexus aurantiacus*) were found to contain three tandem in-frame stop codons.

Pseudoknot 2 (helices 6 and 7)

Pseudoknot 2 was well supported and similar in overall design to pk1. Helical sections 6b and 6c showed a potential to form a continuous helix in *Thermotoga maritima*. In beta-Proteobacteria, 6b was replaced by a short hairpin6d [1]. Helix 6d was observed also in three tmRNAs of the gamma-Proteobacteria *Acidithiobacillus ferrooxidans* and *Francisella tularensis*.

Pseudoknot 3 (helices 8 and 9)

Pseudoknot 3 was well supported but missing in Cyanobacteria and the organelles (Table 1). Helical sections 8a and 8b were likely to be continuously stacked because a single helix was present in some species such as *Aquifex aeolicus*. The unusual purine-rich internal loop between helical sections 8a and 8b was present in most gamma-Proteobacteria suggesting a special function.

Pseudoknot 4 (helices 10 and 11)

This feature was well supported and was similar in design to the other tmRNA pseudoknots. Helical sections 10a and 10b had the potential to stack because a single helix was present in *Prevotella intermedia*. In some Cyanobacteria sequences, however, pk4 was replaced with two smaller tandem pseudoknots.

Secondary structure prediction of the MLD

Because CSA was unable to determine secondary structure for a large portion of the MLD, energy calculations were carried out aimed to predict structure for the single-stranded portion of the open reading frame. The region corresponding to residues 79–107 of *E. coli* tmRNA (Figure 1) was extracted from the alignment. A representative alignment of 197 sequences was submitted to Mfold [29]. Each sequence had the potential to form at least one helix, designated "m" (see Figure 1, additional file 5: Banthracis2D.pdf, and additional file 6: Ccrescentus2D.pdf). Two or more adjacent helices were predicted for 17 sequences. The number of basepairs varied from two in *Chloroflexus aurantiacus* to ten in *Mycoplasma pulmonis*.

Tertiary structure modeling and visualization of tmRNA

ERNA-3D, a program developed to model RNA in three

Secondary structures of three representative tmRNA molecules

Secondary structures were determined for all sequences in the alignment but only three were extracted, diagrammed, and processed for 3-D modeling.

Secondary structure of E. coli tmRNA

The 363-nucleotide tmRNA of the gamma-Proteobacterium *Escherichia coli* represented the typical tmRNA containing the TLD, the MLD, and four pseudoknots (pk1 to pk4) encompassing the pseudoknot domain (PKD). The 90-GCA-92 resume triplet coded for alanine. Two in-frame UAA stop codons (positions 120–125) were located within the terminal loop of helix 5 (Figure 1). Three base-paired regions (shown boxed) were only weakly supported by CSA. Helixm (residues 87–98) was predicted only by energy calculations. A slightly different helix involving residues 88–100 has been suggested by footprinting of *E. coli* tmRNA [30]. The evidence for the 112U-A133 basepair was weak, but was included due to the possibility of extending helix 5 (Materials and Methods). Helical section 5a (residues 108–113 and 134–137) was enlarged by the weakly supported 108G-C137, 110U-A135 and 111U-G134. The 109C-G136 pair was disproved. In helix 10ab, the basepair between 256G-C275 was only weakly supported. Helix 10ab (residues 248–256 and 274–283) could be extended by the boxed 257U-G274 pair.

Secondary structure of Bacillus anthracis tmRNA

Overall, the secondary structure of *Bacillus anthracis* tmRNA (see additional file 5: Banthracis2D.pdf) was similar to that of *E. coli*. One notable difference was a bulged uridine (U57) between helical sections 4a and 4b in pk1. A three-basepair helixm was predicted. The resume triplet (residues 89–91) coded for glycine, and the UAA stop codon was located at residues 119–121. Two weakly-supported pairs (108C-G132 and 109U-A131) extended helical section 5a.

Secondary structure of Caulobacter crescentus tmRNA

Caulobacter crescentus tmRNA (additional file 6: Ccrescentus2D.pdf) consisted of two chains, A and B, of 213 and 83 residues, respectively. The resume codon (82-GCG-84 of chainA) coded for alanine and was followed by a UAA stop codon at residues 121–123. Helical sectionsm1 and m2 were predicted by energy calculations. There was weak support for 5a (G109-U135 and 111C-G133 in chainA), and the 106U-A138, 107U-A137, 108C-G136, and 110C-G134 in chainA were disproved. The pseudoknots were relatively small. Helix 11 corresponded to the absent pk4 (residues 1–18 in chain B).

dimensions [11], was used on an SGI workstation as described in Materials and Methods. *E. coli* tmRNA was

Table 2: Structural motifs used for the *Escherichia coli* tmRNA model

Motif	SCOR class	tmRNA Res.	Source Res.	Coordinates	Comments
1		1–7, 353–363	1–7, 12–22	1IKD.pdb (chain W)	ACCA end and G3-U357 pair
2		8–28, 325–352	8–28, 325–352	tmx-34.pdb from tmRDB	
3a	internal loop with unpaired stacked bases	29–33, 321–324	1775–1779, 1765–1768	1JJ2.pdb	
3b	stacked duplex with one non-WC pair	C35, A319		ERNA-3D	
4	stacked duplex with two non-WC pairs	38–39, 315–316	2874–2875, 2882–2883	1JJ2.pdb	
5		309–311		ERNA-3D	
6a	pseudoknot	49–78	1–33	1RNK.pdb	pk1
6b	tetraloop	87–98	5–8	1AFX.pdb	the only YRRR tetraloop in SCOR
7	nonalooop	118–126	1834–1842	1JJ2.pdb	
8	one unpaired and stacked U	U131	U30	1B36.pdb	
9		171–174		ERNA-3D	
10a	stacked duplex with two non-WC pairs	149–150, 165–166	288–289, 363–364	1JJ2.pdb	
10b	pseudoknot	138–196		6a	pk2
11a	internal loop	204–206, 223–225	780–782, 800–802	1J5E.pdb	
11b	pseudoknot	197–247		6a	pk3
12	stacked duplex with one non-WC pair	G258, A273	A-G6, B-A27	420D.pdb	
13a	stacked duplex with one non-WC pair	C266, U296		ERNA-3D	
13b	pseudoknot	248–299		6a	pk4

Shown in columns one to four are the motif numbers in bold, their SCOR classification [12], the residue positions in the tmRNA model and the source structure. column five lists the filenames containing the atomic coordinates that were derived from the PDB [31], the tmRDB [52], or were generated by ERNA-3D [11].

selected because this tmRNA is the subject of extensive research. *B. anthracis* tmRNA was chosen as an example of a tmRNA from a Gram-positive bacterium, and *C. crescentus* tmRNA was selected it represents a two-part tmRNA.

In order to create the initial models, the sequence and basepairing information were entered into an ERNA-3D input file to automatically generate A-form RNA for the helices sections and specify the single-stranded regions using ERNA-3D's algorithm [11]. Since ERNA-3D avoided an XYZ coordinate system as reference for the user, the manipulation of the model from the viewer's perspective was simple and intuitive. The coordinates of each model were saved in PDB format [31] for compatibility with other molecular modeling programs. Motifs (listed in Tables 2 to 4) were selected to model the loops and turns of a particular tmRNA. ERNA-3D selection files were generated to define clusters and place the motif in 3-D without disturbance to the rest of the model. The 3-D cursor box was used to manipulate a cluster in three-dimensional space, similar to the manipulation of a section of a physical model.

Numerous high-resolution structures determined by NMR or X-ray crystallography represented a rich source of detailed information for defining biologically meaningful motifs. The SCOR database [12] provided a way to find suitable templates. In rare cases when a SCOR search for a

motif did not result in an acceptable match (e.g. motif 9, Table 2), the nucleotides were positioned manually in ERNA-3D. Otherwise, the coordinates were obtained from the Protein Data Bank PDB [32], extracted using the program Swiss-PDBViewer [33], and imported into ERNA-3D. The source motif and the region to be modeled were selected as separate clusters and aligned in three dimensions using common features (usually a shared basepair). Once superimposed, the coordinates of the residues in the source motif were copied onto the corresponding residues in the model. The template was then deleted, leaving a biologically meaningful structure. The backbone connections between the motif and the rest of the model were inspected visually and, if needed, manual adjustments were made to correct bond lengths and tetrahedral angles involving the phosphorous atom at the joint between the extracted motif and the helical structures generated by ERNA-3D.

As an example of the motif modeling process, the purine-rich loop in *E. coli* pk3 (positions 204–206 and 223–225) was constructed using a similar loop in the 30S ribosomal subunit. First, the purine-rich loop was defined as motif 11a (Table 2), and used to search the SCOR database. Positions 780–782 and 800–802 in the structure of the *Thermus thermophilus* 30S ribosomal subunit [34] were found to conform to the motif. The 30S ribosomal subunit coordinates (1J5E.pdb in this case) were downloaded

Table 3: Structural motifs used for the *Bacillus anthracis* tmRNA mode

Motif	SCOR class	tmRNA Res.	Source Res.	Coordinates	Comments
1		1-11, 12-27, 316-355	1-11, 13-28, 324-363	<i>E. coli</i> 1	ACCA end and G3-U349 pair
2	<i>loop with stacked interdigitated bases</i>	28-33, 312-316	477-482, 451-455	IJ5E.pdb	
3		300-301		ERNA-3D	
4a		43-53, 61-65, 294-299	43-53, 63-67, 302-308	<i>E. coli</i> model	helix 2d, helix 3
4b	<i>pseudoknot</i>	58-60, 66, 67-73	12-14, 20, 23-29,	IRNK.pdb	pk1, helix 4b
4c		54-56, 74-75	54-56, 77-78	<i>E. coli</i> 6a	pk1, helix 4a
5	<i>heptaloop</i>	82-88	335-341	IJJ2.pdb	
6a	<i>one looped out A</i>	A112	210	IGID.pdb	
6b		C114, C127		ERNA-3D	
6c	<i>octaloop</i>	117-124	1499-1506	IJJ2.pdb	
7a		134-138, U163, A164, 165-169,	140-144, A171, A174, 175-179	<i>E. coli</i> 10b	helix 6a, looped out U163 and A164.
7b	<i>one looped out U</i>	U158	U87	IJJ2.pdb	
7c		144-147, 148-156, 180-185	259-262, 264-272, 293-298	<i>E. coli</i> 13b	helix 6c, helix 7, pk2
8		G133, C170, 171-177, 178-179	C138, G181, 182-188, 190-191	<i>E. coli</i> 10b	
9a		C190, 191-198, 208-215, 216	G200, 203-210, 219-226, U229	<i>E. coli</i> 11a, 11b	purine-rich loop, pk3
9b	<i>pseudoknot</i>	202-206, 228-232	9-13, 28-32	IRNK.pdb	pk3, helix 9
10a		199-201	154-156	<i>E. coli</i> 6a	pk3
10b		217-227	229-239	<i>E. coli</i> 6a	pk3
11a	<i>one looped out C</i>	C269	C6	IBVJ.pdb	
11b	<i>stacked duplexes with four non-WC pairs</i>	241-245, 260-263	795-798, 815-818	IJJ2.pdb	
12		246-259, 275-290	259-277, 284-299	<i>E. coli</i> 6a	helix 10c, helix 11ab, pk4

Motif numbers in bold, their SCOR classification [12], residue positions in the tmRNA model and the source structure are shown in columns one to four. Column five lists the filenames containing the atomic coordinates that were derived from the PDB [31], the *E. coli* model (see Table 2), or were generated by ERNA-3D [11].

from the PDB and displayed using Swiss-PDBViewer. The coordinates of the loop and the closing basepairs were extracted and inspected to confirm that the structure was compatible. The clustered regions were aligned with the ends of helical sections 8a and 8b at the basepairs 203U-G226 and 207A-U222 of the *E. coli* model and 779C-G803 and 783C-G799 of the template. Template positions 780-AAA-782 and 800-GUA-802 were then copied onto 204-GGA-206 and 223-GAA-225 of the model. The template was deleted and the bond lengths and angles involving the atoms of the phosphates of residues U203, G222, A206, and U222 were adjusted.

In some instances, the tmRNA sequence alignment was reinvestigated using ideas derived from the 3-D model. For example, the alignments of pk1 in *Bacillus anthracis* tmRNA and relatives was changed from a two nucleotide bulge (56-AU-57) between helical sections 4a and 4b to a more feasible and equally well supported one-nucleotide bulge (U57, see additional file 5: Banthracis2D.pdf). The

alignment of helix 10 in pk3 in *B. anthracis* tmRNA and relatives was altered from a 237C-A269 mismatch and an asymmetrical loop (C239 and 266-GU-267) to a single looped-out C269. The alignment of pk3 of *Caulobacter crescentus* and relatives was changed from four basepairs and a weakly supported fifth pair in helix 8 (between 174G-C196 of chainA) to the four basepair structure seen in additional file 6: Ccrescentus2D.pdf. Information about spatial neighborhoods as obtained from cross-linking, site-directed mutagenesis, and functional testing of *E. coli* tmRNA was introduced and is described in detail below. All models were inspected visually for correct bond angles and distances around the phosphorous atoms at the joints between the extracted motifs and the helical regions generated by ERNA-3D. The coordinates are provided as additional file 7: Ecoli-closed.pdb, 8: Ecoli-open.pdb, 9: Banthracis-closed.pdb, and 10: Ccrescentus-closed.pdb.

Table 4: Structural motifs used for the *Caulobacter crescentus* tmRNA model

Motif	SCOR class	tmRNA Res.	Source Res.	Coordinates	Comments
1		A-1-13, A-14-21, B-50-83	1-13, 15-22, 322-355.	<i>B. anthracis</i> 1	-
2a	one non-Watson Crick pair and one looped-out A	A-22, B-48-49	14, 4-5	5MSF.pdb	disruption in anticodon stem
2b	loop with base triple	A-26-31; B-40-44	8-13, 24-28	1FMN.pdb	
2c		A-C36, B-C35		ERNA-3D	
3		A-40-41, B-27-31		ERNA-3D	
4		A-47-61, A-62-70	196-210, 224-232	<i>B. anthracis</i> 8a, 8b, 9a, 9c	pk1
5		A-87-93	82-88	<i>B. anthracis</i> 5	terminal heptaloop of helix m2
6	one looped out A and one or more non-WC pairs	A-78-81, A-99-101	113-116, 205-207	1GID.pdb	internal loop between helices m1 and m2
7		B-8-11	284-285, 291-292	1D6K.pdb	
8a		A-112-114, A-131-132		ERNA-3D	
8b		A-119-125	82-88	<i>B. anthracis</i> 5	
9a		U148, C163		ERNA-3D	
9b		A-156-165, A-146-153, A-167-171	157-166, 149-156, 192-196	<i>E. coli</i> 10b	pk2. Single-stranded regions were adjusted to connect helices
10		A-154-156, A-170-171	54-55, 76-77	<i>E. coli</i> 6a	Correction of two pairs in pk2 based on <i>E. coli</i> pk1
11		A-211-214, A-177-182, A-184-193, A-177-178, A-192-198, A-194-209	360-363, 207-212, 213-222, 200-201, 228-234, 230-245	<i>E. coli</i> 1 (ACCU tail) and 11b	pk3 and ACCU tail of pk3

Motif numbers in bold, their SCOR classification [12], residue positions in the tmRNA model and the source structure are shown in columns one to four. Column five lists the filenames containing the atomic coordinates that were derived from the PDB [31], the *E. coli* or *B. anthracis* models (see Tables 2 and 3), or were generated by ERNA-3D [11].

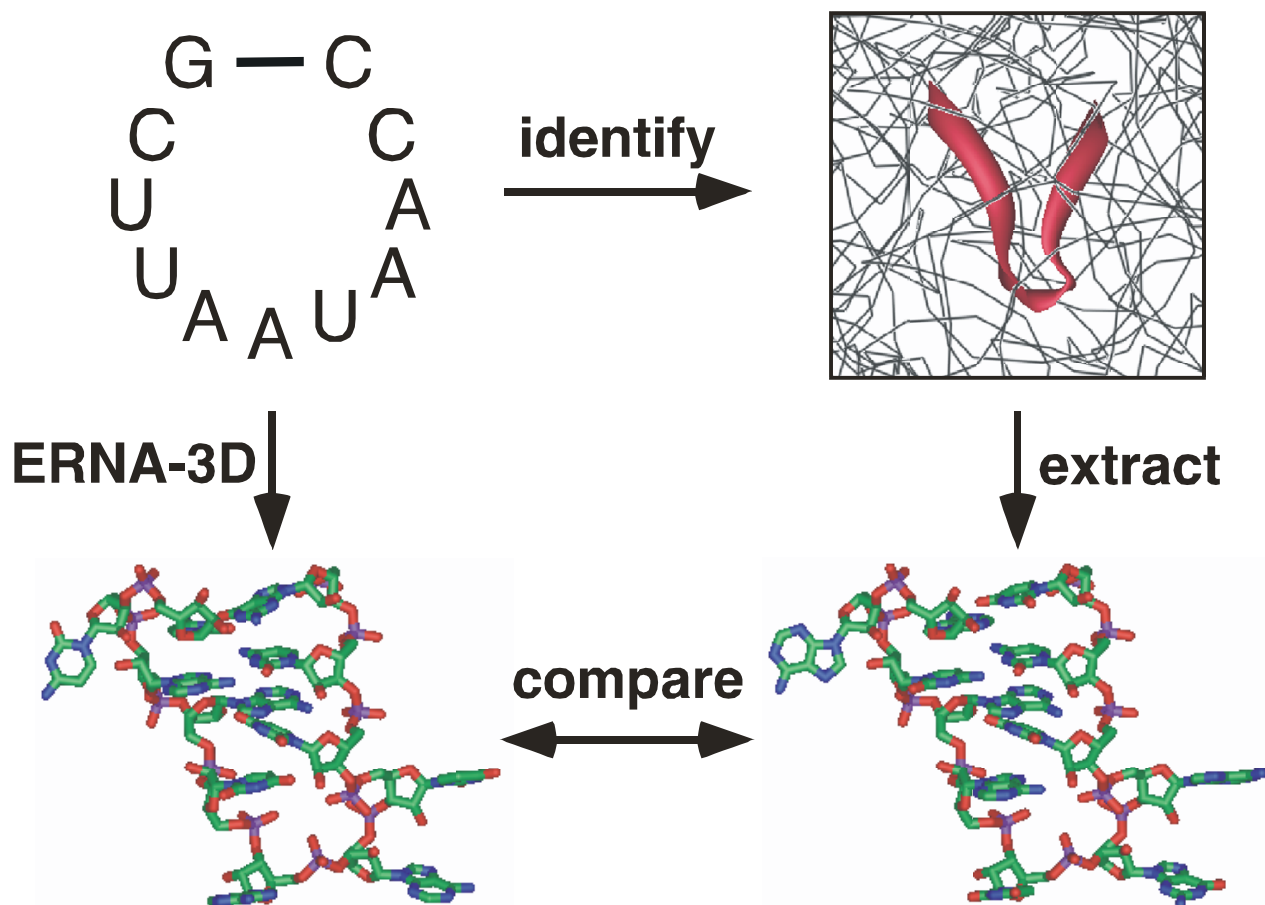
3-D model of *E. coli* tmRNA

The model shown as a ribbon diagram in Figure 3 consists of a compacted MLD and PKD with the TLD extending from the body of the molecule due to the near-coaxial stacking of the helix 2 sections. The coordinates for the TLD were taken from a previous model [35] which is based on two cross-linked sites, one formed between nucleotides U9/U10 near the 5' end and nucleotides C346/U347 in the T loop, the other involving residues at positions 25-28 and 326-329 within helix 2a (motif 2 in Table 2). Important features of the TLD include the non-Watson-Crick base pairs formed by 19-GA-20 and 333-GA-334 which have been confirmed by site-directed mutagenesis [36].

A very efficient UV-induced cross-link observed between the stop codon loop of helix 5 and pk2 of *E. coli* tmRNA (Wower et al., unpublished) introduced a considerable constraint of helices 5, 6, and 7, and, as has been shown recently, is consistent with the cryo-EM structure of ribosome-bound tmRNA of the initial stage of *trans*-translation [10]. Also considered was the previously-discovered covariation [37] between C44 and C66 (*E. coli* numbering, Figure 1) which determines the orientation of helix 2 in

relation to helix 3 and thus the approximate angle by which the TLD protrudes. The 44/66 covariation is strongly supported (26 covariations *versus* four mismatches) in an alignment of 143 representative sequences (not shown). Since this is a non-Watson-Crick covariation, it is difficult to propose a precise structure in this region. More extensive studies will be required to better understand the nature of the 44/66 covariation.

Overall, the distance between the 3'end and A231 in pk3 was 180 Å, and 70 Å between the outside edges of pk1 and pk4. Helix 5 and pk2 were positioned in a parallel fashion. The nucleotides in the bulge between helical sections 6a and 6b (motif 9, Table 2) were adjusted manually to allow for a close fit of helix 5 and pk2. This model is supported by the finding that mutations that destroy base pairing in helix 5 substantially decrease tmRNA tagging activity (Wower et al, in press) and abolish the long-distance interaction between helix 5 and pk2 as judged by the absence of a cross-link between the stop codon loop of helix 5 and pk2 (Wower, unpublished data). Evidence for the existence of helix 5 has been provided by the analysis of compensatory mutations which completely restore tagging [28]. Each of the four pseudoknots displayed the

**Figure 2**

Motif modeling procedure. Motifs, for example the nonamer-loop shown in the top-left panel, were identified in the known high-resolution structures (top-right) with the help of SCOR [12]. The PDB coordinates were extracted (bottom-right) and compared with the 3-D model generated by ERNA-3D (bottom-left) to deduce relevant models.

previously determined structural properties characterized by extensive helical stacking [27]. The MLD and pseudoknots were arranged in a central loop with the resume codon positioned near the junction between helices 2a and 2b (motif 3a, Table 2). Our model reflects the finding that the pseudoknots are functionally interchangeable [38] and thus are likely to retain a considerable level of structural independence. Furthermore, data derived from cross-linking experiments showing that pk2 and pk3 are in close proximity whereas helix 5 and pk4 are further apart (Wower, unpublished data) agree with the presented model.

3-D model of *B. anthracis* tmRNA

The 3-D model of the *B. anthracis* tmRNA (Figure 4) was similar to the *E. coli* model. A sharper angle was modeled between helix 2 axis and the PKD. The dimensions were 150 Å from the 3' end to the distant edge of pk2, and approximately 80 Å between the outer edges of pk2 and pk4, respectively.

3-D model of *C. crescentus* two-part tmRNA

Compared to the other two tmRNA models, the two-part tmRNA *Caulobacter crescentus* model (Figure 5) was slightly more elongated. It measured 195 Å from the 3'-

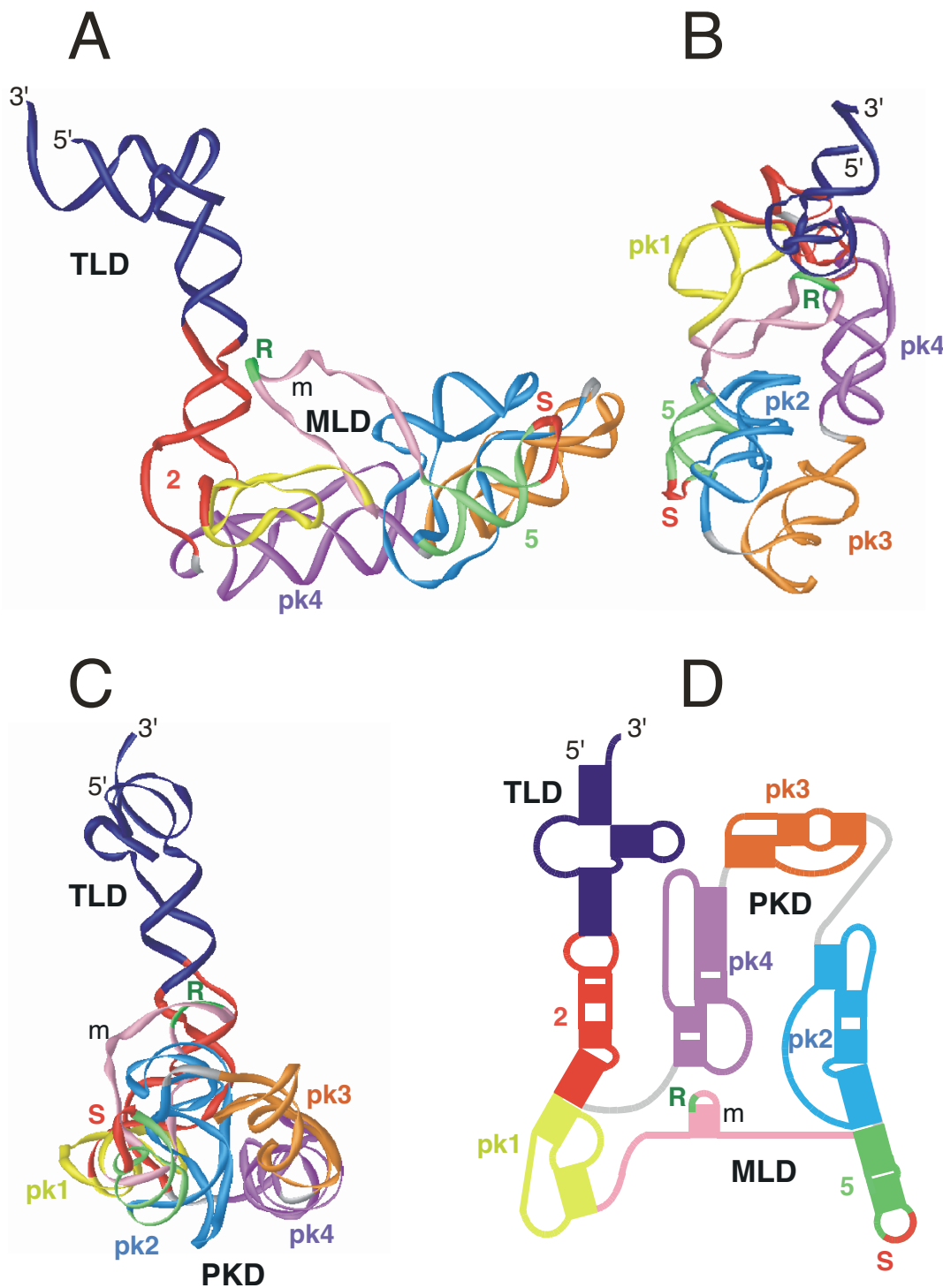


Figure 3

3-D model of *Escherichia coli* tmRNA. The 3-D model of *Escherichia coli* tmRNA is viewed as a ribbon diagram from the side in panel A, the top in panel B, and in panel C turned by approximately 90° around the y-axis in relation to A. Panel D shows a representation of the corresponding 2-D structure using the identical coloring scheme. Labeled are the 5' and 3' ends, the resume (R) and stop codons (S), and the three domains (TLD, MLD, PKD). The figure was produced with iMol [53] and the PDB coordinates of additional file 7: Ecoli-closed.pdb.

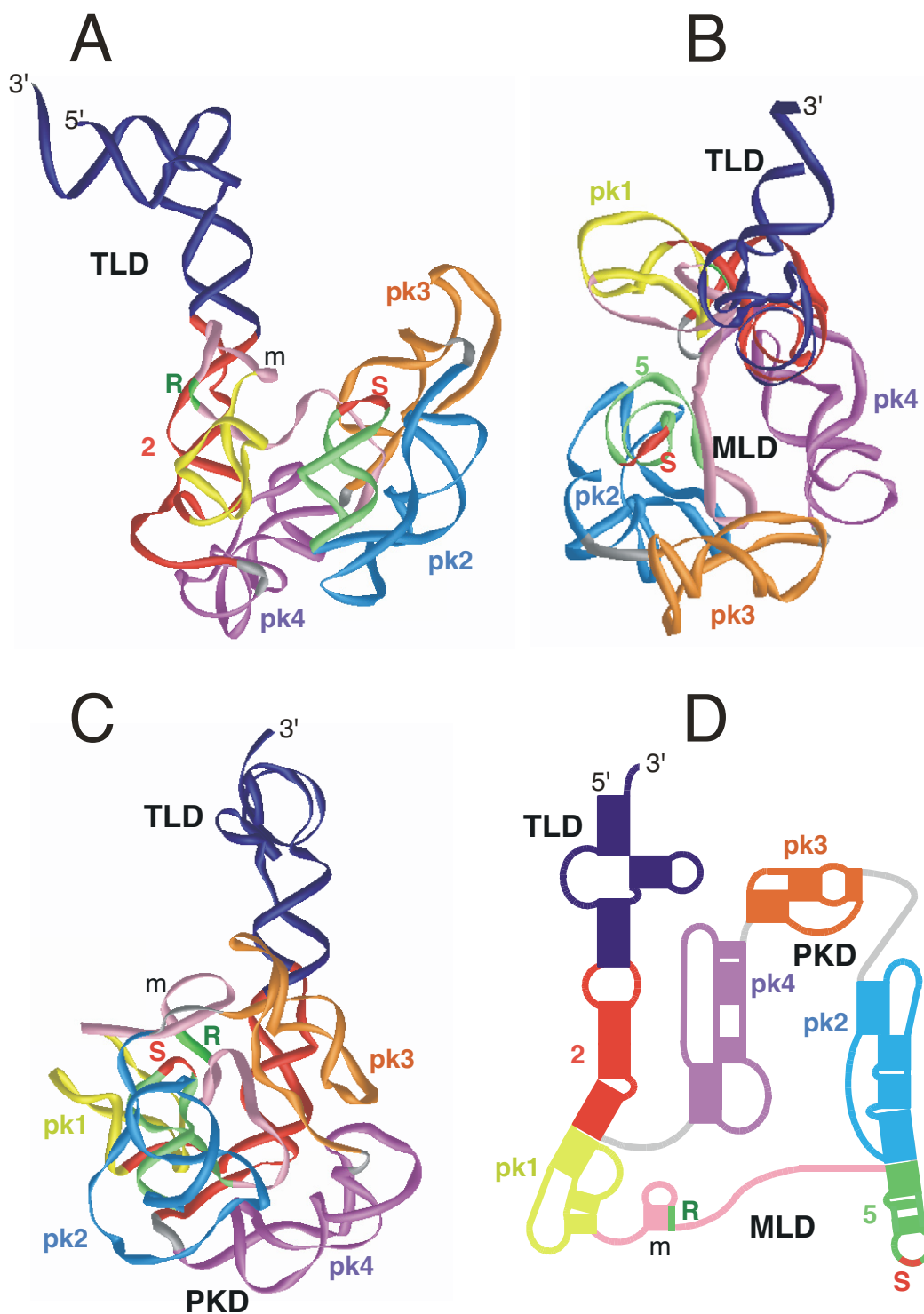


Figure 4
3-D model of *Bacillus anthracis* tmRNA. The 3-D model of *Bacillus anthracis* tmRNA is viewed as a ribbon diagram from the side in panel A, the top in panel B, and in panel C turned by approximately 90° around the y-axis in relation to A. Panel D shows a representation of the corresponding 2-D structure using the identical coloring scheme. Labeled are the 5' and 3' ends, the resume (R) and stop codons (S), and the three domains (TLD, MLD, PKD). The figure was produced with iMol [53] and the PDB coordinates of additional file 9: Banthraxis-closed.pdb.

end of chainB to the single-stranded region between pk2 and pk3. The distance between helix 5 and the 3'end of chainA was 55 Å.

Discussion

We have compared a growing number of tmRNA sequences from all groups of bacteria to produce an alignment from which the secondary structure of any tmRNA could be easily extracted. Most basepairs were supported by phylogenetic evidence, whereas only a few helical sections required energy calculations. Uncertainties in assignment of basepairs, such as the pseudoknot region of chloroplasts and one-piece cyanobacterial tmRNAs, may be eliminated in the future when more sequences will become available.

The common layout of the secondary structures indicated a similar function in all bacteria. The number and size of the pseudoknots varied, supporting the idea that the pseudoknots may only enhance the essential functions carried by the TLD and the MLD [28]. Differences in the secondary structure features were usually not random but occurred between groups of related organisms. For example, helix 6d was present only in the beta- and three close relatives of the gamma-Proteobacteria. Whether these group-specific features are responsible for differences in the *trans*-translation mechanism remains to be determined. However, strategies that exploit these differences, for example for developing new antibiotics targeted at a specific group of bacteria, can now be envisioned.

In principle, tertiary structure models of any tmRNA in the alignment could be built using the described procedures. Here, we have shown how to generate a biologically more meaningful model of *E. coli* tmRNA which represents a significant progress from a previous model [27]. We also constructed 3-D model of the tmRNAs of *B. anthracis* and *C. crescentus*. Overall, the three models were similar in shape and size confirming that all tmRNAs have the potential to function similarly in *trans*-translation. The TLD mimicked the L-shape of canonical tRNA [39] and may be necessary for proper association tmRNA with the EF-Tu, SmpB, and subsequent binding to the ribosomal A-site. The lack of a D-stem has been suggested to confer flexibility [40], but SmpB may be responsible for stabilizing this region [41,42].

Differences in the shapes of the three tmRNA models (e.g. the angle between helix 2 and the main body of the molecule) may be due to the difficulty in determining the precise arrangement of the pseudoknots. Considering that the pseudoknots are likely to constitute relatively independent structural units, conformational changes might occur around the connecting single strands, as well as in the MLD and the weakly-supported helix m. TmRNA may

become less flexible when bound to proteins such as SmpB and ribosomal protein S1. EF-Tu, however, likely binds to the coaxially-stacked helices 1 and 12 [43], and therefore appears to have little effect on the conformation of the TLD. Protein SmpB was found to bind near helix 2a [41,44], has two RNA binding sites [45], and thus could make additional contacts with other regions. Protein S1 is the largest ribosomal protein, has been shown to be close to numerous sites, and to be required for the binding of tmRNA to the ribosome [7]. Since S1 is a flexible, beadlike protein [46] it may not restrict the conformational potential of the tmRNA molecule. Instead, the protein may instill some constraint to the large central loop formed by the PKD and the MLD. Because S1 is known to melt helices in mRNAs [47], it is also possible that it unwinds helix m and exposes the resume codon and the preceding nucleotides U85 and A86 for efficient *trans*-translation [48,49].

The tmRNA models show the resume codon in close proximity to the internal loop formed between helical sections 2a and 2b. This arrangement would allow the ribosome to "jump" a relatively short distance from the end of the broken mRNA onto the ORF of tmRNA. In a recent cryo-EM study of the initial stage of *trans*-translation [10], the tRNA-like region, SmpB, EF-Tu, and part of pk4 were located in the A-site of the ribosome. We suggest that this more open arrangement is made possible due to the flexibility of tmRNA, the melting of helix m, and/or a change in conformation induced by the binding of tmRNA to the ribosome (Figure 6). The opening of the central loop seems to be accompanied by a rotation of the TLD around the helix 2 axis (compare Figure 6A and 6B) and thus might properly align the resume codon with the 3'-end of broken mRNA in the ribosomal decoding centre. At the later stages of the transit of tmRNA across the ribosome even more dramatic conformational changes were shown to disrupt helix 5 and the pseudoknotted regions (Wower et al, in press). These downstream alterations are likely mediated not by protein S1 but by the intrinsic helicase activity of the ribosome [50] and are required to maintain the ribosomal subunits in close proximity to the unfolded tmRNA in order to monitor *trans*-translation.

Conclusion

This study significantly advances our understanding of *trans*-translation by providing biologically feasible 3-D models for the entire tmRNA molecule. Although the modeling of only three tmRNAs has been described here, 3-D models of every tmRNA can be extracted from the alignment. The models are characterized by a functionally significant features, including biologically relevant structures for the single-stranded regions and the close proximity between the TLD and the resume codon. Conformational changes induced by binding of tmRNA

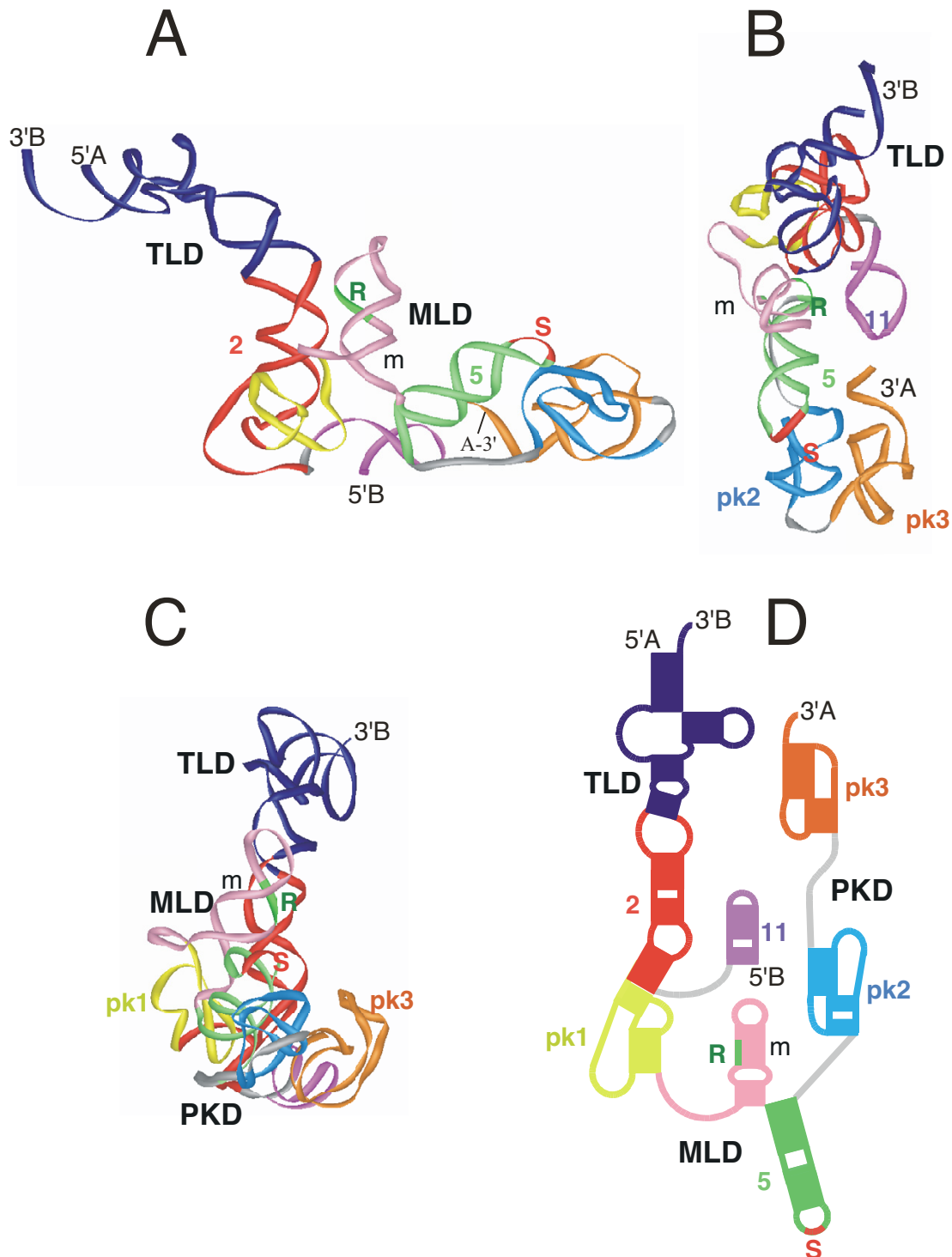


Figure 5
3-D model of *Caulobacter crescentus* tmRNA. The 3-D model of *Caulobacter crescentus* s tmRNA is viewed as a ribbon diagram from the side in panel A, the top in panel B, and in panel C turned by approximately 90° around the y-axis in relation to A. Panel D shows a representation of the corresponding 2-D structure using the identical coloring scheme. Labeled are the 5' and 3' ends, the resume (R) and stop codons (S), and the three domains (TLD, MLD, PKD). The figure was produced with iMol [53] and the PDB coordinates of additional file 10: Ccrescentus-closed.pdb.

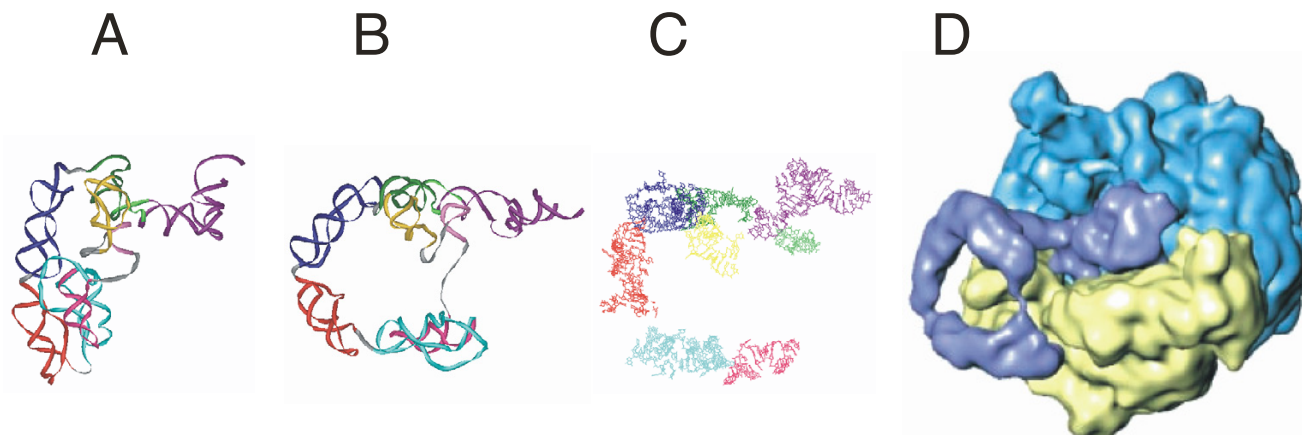


Figure 6

Conformational changes in *Escherichia coli* tmRNA. Panel A: closed form of the *E. coli* model as shown in Figure 3. Panel B: open conformation adjusted to more closely resemble the ribosome-bound form as determined by cryo-EM [10] using additional file 8: Ecoli-open.pdb. Panel C: coordinates extracted from the cryo-EM model [10]. The TLD is shown in dark purple, helix 2 in green, pk1 in yellow, helix 5 in pink, pk2 in turquoise, pk3 in red, and pk4 in dark blue. Panel D: Electron density map of the 50S subunit in light blue, the 30S subunit in yellow, and the bound tmRNA (in the absence of ribosomal protein S1) in dark blue (from [10]).

to SmpB, ribosomal protein S1, and the ribosome suggest a transformation of a free compact tmRNA to a more open ribosome-bound structure. The comparative modeling approach described here for tmRNA is easily adapted for other RNA classes.

Methods

Comparative sequence analysis

The tmRNA sequences were arranged in phylogenetic order using information available in the RDP [19]. When the phylogenetic order could not be determined, the sequence was placed next to the closest relative as determined by the ClustalW plug-in of BioEdit [18,51]. The sequences were made available at the tmRDB [52].

Aligning was done manually using BioEdit [18] with details described previously [13]. Briefly, closely related sequences were aligned first. Then, invariant positions were used as guides to align the dissimilar regions. Next, common secondary structure elements were identified by observing covariations and find support for basepairs, tertiary interactions, or other structural features. Compensatory base changes (CBCs) were observed if a change in one residue of a Watson-Crick or G-U pair was compensated by a second change to maintain basepairing. Two residues were mismatched if they did not form a Watson-Crick or G-U pair. CBCs and mismatches were counted to determine positive and negative evidence in

order to prove or disprove the existence of a particular pair. A basepair was considered proven if there was at least twice as much positive than negative evidence. Invariant pairs provided neither positive nor negative evidence. If a basepair was proven in one phylogenetic group and disproven in another group, the basepair was considered to be specific to that group.

The alignment and suggested CBCs were checked using RNAdbTools [22] to eliminate incorrectly-paired nucleotides, suggest extensions of helices, and determine the phylogenetic support for each basepair. Weakly supported basepairs adjacent to supported basepairs were considered an extension of the helix and usually included in the secondary structures (Figure 1, additional file 5: Banthracis2D.pdf and 6: Ccrescentus2D.pdf).

3-D model building

The secondary structure information was used as input for ERNA-3D [11] installed on an SGI workstation running IRIX 6.5. ERNA-3D generated A-form RNA for each helix and calculated the conformations of single-stranded regions. The models were examined using CrystalEyes stereovision goggles and an StereoGraphics infrared emitter. Structural motifs were identified using SCOR [12], the coordinates were obtained from the Protein Data Bank (PDB) [32], extracted using Swiss-PDBViewer [33], and superimposed onto the model. Data obtained from site-

directed mutagenesis, cross-linking experiments, or the literature were incorporated, and bond lengths and angles were adjusted manually to produce biologically feasible models. The final models were saved in PDB format (additional files 7: Ecoli-closed.pdb, 8: Ecoli-open.pdb, 9: Banthracis-closed.pdb, and 10: Ccrescentus-closed.pdb and viewed in iMol [53] to create the ribbon diagrams shown in Figures 3 to 5.

Authors' contributions

JB identified and aligned a large number of the tmRNA sequences, carried out the 3-D modeling experiments, and drafted portions of the text. CZ conceived the study, participated in all of its aspects, and wrote the final manuscript. FM developed the ERNA-3D program and incorporated new functions to allow comparative modeling of RNA. IW developed assays which allowed to test the biological significance of the *Escherichia coli* tmRNA model. JW participated in the coordination of the study and provided RNA-RNA cross-link data which were crucial for constraining the models in 3-D. All authors read and approved the final manuscript.

Additional material

Additional File 1

tmRNA alignment. Species names are shown on the left with their tmRDB ID (see <http://psyche.uthct.edu/dbs/tmRDB/tmRDB.html>). Supported base pairing are shown with upper case letters and are indicated on the bottom. Secondary structure features are indicated on the top.

Click here for file

[<http://www.biomedcentral.com/content/supplementary/1471-2199-6-14-S1.html>]

Additional File 2

tmRNA alignment. Species names are shown on the left with their tmRDB ID (see <http://psyche.uthct.edu/dbs/tmRDB/tmRDB.html>). Supported base pairing are shown with upper case letters and are indicated on the bottom. Secondary structure features are indicated on the top. Each sequence is shown on a single long line suitable for import into other programs.

Click here for file

[<http://www.biomedcentral.com/content/supplementary/1471-2199-6-14-S2.txt>]

Additional File 3

tmRNA alignment. Species names are shown on the left with their tmRDB ID (see <http://psyche.uthct.edu/dbs/tmRDB/tmRDB.html>). Supported base pairing are shown with upper case letters and are indicated on the bottom. Secondary structure features are indicated on the top. The alignment is shown in sections for easier viewing and printing. This arrangement is not suited for import into other programs.

Click here for file

[<http://www.biomedcentral.com/content/supplementary/1471-2199-6-14-S3.txt>]

Additional File 4

tmRNA alignment. tmRNA alignment in msf format suitable for import into editors which support the msf format. Can be used to convert into other sequence formats using, for example the Readseq server at <http://bio.web.pasteur.fr/seqanal/interfaces/readseq.html>

Click here for file

[<http://www.biomedcentral.com/content/supplementary/1471-2199-6-14-S4.msff>]

Additional File 5

Secondary structure of Bacillus anthracis tmRNA. Phylogenetically-supported helices are highlighted in gray and numbered from 1 to 12. The 5' and 3' ends are indicated. Arrows represent connections from 5' to 3'. Residues are numbered in increments of ten. Weakly supported regions and basepairs are show in boxes. The star labels the first nucleotide of the resume codon. The tag peptide sequence is shown below the mRNA-like region. The stop codon is indicated with a solid arrowheads. Three domains are distinguished: The tRNA-like domain (TLD), the mRNA-like domain (MLD), and the pseudoknot domain (PKD).

Click here for file

[<http://www.biomedcentral.com/content/supplementary/1471-2199-6-14-S5.pdf>]

Additional File 6

Secondary structure of Caulobacter crescentus tmRNA. Phylogenetically-supported helices are highlighted in gray and numbered from 1 to 12. The 5' and 3' ends of both chains are indicated. Arrows represent connections from 5' to 3'. Residues are numbered in increments of ten.

Weakly supported regions and basepairs are show in boxes. The star labels the first nucleotide of the resume codon. The tag peptide sequence is shown below the mRNA-like region. The stop codons are indicated with solid arrowheads. Three domains are distinguished: The tRNA-like domain (TLD), the mRNA-like domain (MLD), and the pseudoknot domain (PKD).

Click here for file

[<http://www.biomedcentral.com/content/supplementary/1471-2199-6-14-S6.pdf>]

Additional File 7

PDB coordinates of the closed form of Escherichia coli tmRNA. 3-D model of the closed form of Escherichia coli tmRNA.

Click here for file

[<http://www.biomedcentral.com/content/supplementary/1471-2199-6-14-S7.pdb>]

Additional File 8

PDB coordinates of the open form of Escherichia coli tmRNA. 3-D model of the open form of Escherichia coli tmRNA.

Click here for file

[<http://www.biomedcentral.com/content/supplementary/1471-2199-6-14-S8.pdb>]

Additional File 9

PDB coordinates of the closed form of Bacillus anthracis tmRNA. 3-D model of the open form of Bacillus anthracis tmRNA.

Click here for file

[<http://www.biomedcentral.com/content/supplementary/1471-2199-6-14-S9.pdb>]

Additional File 10

PDB coordinates of the closed form of *Caulobacter crescentus* tmRNA.

3-D model of the closed form of *Caulobacter crescentus* tmRNA.

Click here for file

[<http://www.biomedcentral.com/content/supplementary/1471-2199-6-14-S10.pdf>]

Acknowledgements

This work was supported by Grant GM58267 to JW from the National Institutes of Health.

References

- Zwieb C, Wower I, Wower J: **Comparative sequence analysis of tmRNA.** *Nucleic Acids Res* 1999, **27(10)**:2063-2071.
- Withey J, Friedman D: **Analysis of the role of trans-translation in the requirement of tmRNA for lambda daimmP22 growth in Escherichia coli.** *J Bacteriol* 1999, **181(7)**:2148-2157.
- Tu GF, Reid GE, Zhang JG, Moritz RL, Simpson RJ: **C-terminal extension of truncated recombinant proteins in Escherichia coli with a 10Sa RNA decapeptide.** *J Biol Chem* 1995, **270(16)**:9322-9326.
- Keiler KC, Waller PR, Sauer RT: **Role of a peptide tagging system in degradation of proteins synthesized from damaged messenger RNA.** *Science* 1996, **271(5251)**:990-993.
- Himeno H, Sato M, Tadaki T, Fukushima M, Ushida C, Muto A: **In vitro trans translation mediated by alanine-charged 10Sa RNA.** *J Mol Biol* 1997, **268(5)**:803-808.
- Karzai AW, Roche ED, Sauer RT: **The SsrA-SmpB system for protein tagging, directed degradation and ribosome rescue.** *Nat Struct Biol* 2000, **7(6)**:449-455.
- Wower IK, Zwieb CW, Guven SA, Wower J: **Binding and cross-linking of tmRNA to ribosomal protein S1, on and off the Escherichia coli ribosome.** *Embo J* 2000, **19(23)**:6612-6621.
- Barends S, Wower J, Kraal B: **Kinetic parameters for tmRNA binding to alanyl-tRNA synthetase and elongation factor Tu from Escherichia coli.** *Biochemistry* 2000, **39(10)**:2652-2658.
- Karzai AW, Sauer RT: **Protein factors associated with the SsrA-SmpB tagging and ribosome rescue complex.** *Proc Natl Acad Sci U S A* 2001, **98(6)**:3040-3044.
- Valle M, Gillet R, Kaur S, Henne A, Ramakrishnan V, Frank J: **Visualizing tmRNA entry into a stalled ribosome.** *Science* 2003, **300(5616)**:127-130.
- Mueller F, Doring T, Erdemir T, Greuer B, Junke N, Osswald M, Rinke-Appel J, Stade K, Thamm S, Brimacombe R: **Getting closer to an understanding of the three-dimensional structure of ribosomal RNA.** *Biochem Cell Biol* 1995, **73(11-12)**:767-773.
- Klosterman PS, Tamura M, Holbrook SR, Brenner SE: **SCOR: a Structural Classification of RNA database.** *Nucleic Acids Res* 2002, **30(1)**:392-394.
- Larsen N, Zwieb C: **SRP-RNA sequence alignment and secondary structure.** *Nucleic Acids Res* 1991, **19(2)**:209-215.
- Williams KP: **The tmRNA Website: invasion by an intron.** *Nucleic Acids Res* 2002, **30(1)**:179-182.
- Benson DA, Karsch-Mizrachi I, Lipman DJ, Ostell J, Wheeler DL: **GenBank.** *Nucleic Acids Res* 2005, **33 Database Issue**:D34-8.
- Altschul SF, Gish W, Miller W, Myers EV, Lipman DJ: **Basic local alignment search tool.** *J Mol Biol* 1990, **215(3)**:403-410.
- Altschul SF, Madden TL, Schaffer AA, Zhang J, Zhang Z, Miller W, Lipman DJ: **Gapped BLAST and PSI-BLAST: a new generation of protein database search programs.** *Nucleic Acids Res* 1997, **25(17)**:3389-3402.
- Hall TA: **BioEdit: a user-friendly biological sequence alignment editor and analysis program for Windows 95/98/NT.** *Nucl Acids Symp Ser* 1999, **41**:95-98.
- Cole JR, Chai B, Marsh TL, Farris RJ, Wang Q, Kulam SA, Chandra S, McGarrell DM, Schmidt TM, Garrity GM, Tiedje JM: **The Ribosomal Database Project (RDP-II): previewing a new autoaligner that allows regular updates and the new prokaryotic taxonomy.** *Nucleic Acids Res* 2003, **31(1)**:442-443.
- Wheeler DL, Church DM, Federhen S, Lash AE, Madden TL, Pontius JU, Schuler GD, Schriml LM, Sequeira E, Tatusova TA, Wagner L: **Database resources of the National Center for Biotechnology.** *Nucleic Acids Res* 2003, **31(1)**:28-33.
- Keiler KC, Shapiro L, Williams KP: **tmRNAs that encode proteolysis-inducing tags are found in all known bacterial genomes: A two-piece tmRNA functions in Caulobacter.** *Proc Natl Acad Sci U S A* 2000, **97(14)**:7778-7783.
- Gorodkin J, Zwieb C, Knudsen B: **Semi-automated update and cleanup of structural RNA alignment databases.** *Bioinformatics* 2001, **17(7)**:642-645.
- tmRDB. :[<http://psyche.uthct.edu/dbs/tmRDB/>].
- Hou YM, Schimmel P: **A simple structural feature is a major determinant of the identity of a transfer RNA.** *Nature* 1988, **333(6169)**:140-145.
- Komine Y, Kitabatake M, Yokogawa T, Nishikawa K, Inokuchi H: **A tRNA-like structure is present in 10Sa RNA, a small stable RNA from Escherichia coli.** *Proc Natl Acad Sci U S A* 1994, **91(20)**:9223-9227.
- Ushida C, Himeno H, Watanabe T, Muto A: **tRNA-like structures in 10Sa RNAs of Mycoplasma capricolum and Bacillus subtilis.** *Nucleic Acids Res* 1994, **22(16)**:3392-3396.
- Zwieb C, Mueller F, Wower J: **Comparative three-dimensional modeling of tmRNA.** *Nucl Acids Symp Ser* 1999, **41**:200-204.
- Wower IK, Zwieb C, Wower J: **Contributions of pseudoknots and protein SmpB to the structure and function of tmRNA in trans-translation.** *J Biol Chem* 2004, **279(52)**:54202-54209.
- Zuker M: **Mfold web server for nucleic acid folding and hybridization prediction.** *Nucleic Acids Res* 2003, **31(13)**:3406-3415.
- Felden B, Himeno H, Muto A, McCutcheon JP, Atkins JF, Gesteland RF: **Probing the structure of the Escherichia coli 10Sa RNA (tmRNA).** *Rna* 1997, **3(1)**:89-103.
- Sussman JL, Abola EE, Lin D, Jiang J, Manning NO, Prilusky J: **The protein data bank. Bridging the gap between the sequence and 3D structure world.** *Genetica* 1999, **106(1-2)**:149-158.
- Berman HM, Westbrook J, Feng Z, Gilliland G, Bhat TN, Weissig H, Shindyalov IN, Bourne PE: **The Protein Data Bank.** *Nucleic Acids Res* 2000, **28(1)**:235-242.
- Guex N, Peitsch MC: **SWISS-MODEL and the Swiss-PdbViewer: an environment for comparative protein modeling.** *Electrophoresis* 1997, **18(15)**:2714-2723.
- Wimberly BT, Brodersen DE, Clemons WMJ, Morgan-Warren RJ, Carter AP, Vonnrhein C, Hartsch T, Ramakrishnan V: **Structure of the 30S ribosomal subunit.** *Nature* 2000, **407(6802)**:327-339.
- Zwieb C, Guven SA, Wower IK, Wower J: **Three-dimensional folding of the tRNA-like domain of Escherichia coli tmRNA.** *Biochemistry* 2001, **40(32)**:9587-9595.
- Hanawa-Suetsugu K, Bordeau V, Himeno H, Muto A, Felden B: **Importance of the conserved nucleotides around the tRNA-like structure of Escherichia coli transfer-messenger RNA for protein tagging.** *Nucleic Acids Res* 2001, **29(22)**:4663-4673.
- Kelley ST, Harris JK, Pace NR: **Evaluation and refinement of tmRNA structure using gene sequences from natural microbial communities.** *Rna* 2001, **7(9)**:1310-1316.
- Nameki N, Tadaki T, Himeno H, Muto A: **Three of four pseudoknots in tmRNA are interchangeable and are substitutable with single-stranded RNAs.** *FEBS Lett* 2000, **470(3)**:345-349.
- Sussman JL, Holbrook SR, Warrant RW, Church GM, Kim SH: **Crystal structure of yeast phenylalanine transfer RNA. I. Crystallographic refinement.** *J Mol Biol* 1978, **123(4)**:607-630.
- Stagg SM, Frazer-Abel AA, Hagerman PJ, Harvey SC: **Structural studies of the tRNA domain of tmRNA.** *J Mol Biol* 2001, **309(3)**:727-735.
- Barends S, Karzai AW, Sauer RT, Wower J, Kraal B: **Simultaneous and functional binding of SmpB and EF-Tu-TP to the alanyl acceptor arm of tmRNA.** *J Mol Biol* 2001, **314(1)**:9-21.
- Gutmann S, Haebel PV, Metzinger L, Sutter M, Felden B, Ban N: **Crystal structure of the transfer-RNA domain of transfer-messenger RNA in complex with SmpB.** *Nature* 2003, **424(6949)**:699-703.
- Nissen P, Kjeldgaard M, Thirup S, Polekhina G, Reshetnikova L, Clark BF, Nyborg J: **Crystal structure of the ternary complex of Phe-tRNAPhe, EF-Tu, and a GTP analog [see comments].** *Science* 1995, **270(5241)**:1464-1472.

44. Wower J, Zwieb CW, Hoffman DW, Wower IK: **SmpB: a protein that binds to double-stranded segments in tmRNA and tRNA.** *Biochemistry* 2002, **41(28)**:8826-8836.
45. Dong G, Nowakowski J, Hoffman DV: **Structure of small protein B: the protein component of the tmRNA-SmpB system for ribosome rescue.** *Embo J* 2002, **21(7)**:1845-1854.
46. Subramanian AR: **Structure and functions of ribosomal protein S1.** *Prog Nucleic Acid Res Mol Biol* 1983, **28**:101-142.
47. Bear DG, Ng R, Van Derveer D, Johnson NP, Thomas G, Schleich T, Noller HF: **Alteration of polynucleotide secondary structure by ribosomal protein S1.** *Proc Natl Acad Sci U S A* 1976, **73(6)**:1824-1828.
48. Williams KP, Martindale KA, Bartel DP: **Resuming translation on tmRNA: a unique mode of determining a reading frame.** *Embo J* 1999, **18(19)**:5423-5433.
49. Ivanov PV, Zvereva MI, Shpanchenko OV, Dontsova OA, Bogdanov AA, Aglyamova GV, Lim VI, Teraoka Y, Nierhaus KH: **How does tmRNA move through the ribosome?** *FEBS Lett* 2002, **514(1)**:55-59.
50. Takyar S, Hickerson RP, Noller HF: **mRNA helicase activity of the ribosome.** *Cell* 2005, **120(1)**:49-58.
51. Thompson JD, Higgins DG, Gibson TJ: **CLUSTAL W: improving the sensitivity of progressive multiple sequence alignment through sequence weighting, position-specific gap penalties and weight matrix choice.** *Nucleic Acids Res* 1994, **22(22)**:4673-4680.
52. Zwieb C, Gorodkin J, Knudsen B, Burks J, Wower J: **tmRDB (tmRNA database).** *Nucleic Acids Res* 2003, **31(1)**:446-447.
53. **iMol.** :[<http://www.pirx.com/imol>].
54. **Chime.** :[<http://www.umass.edu/microbio/chime/>].

Publish with **BioMed Central** and every scientist can read your work free of charge

"BioMed Central will be the most significant development for disseminating the results of biomedical research in our lifetime."

Sir Paul Nurse, Cancer Research UK

Your research papers will be:

- available free of charge to the entire biomedical community
- peer reviewed and published immediately upon acceptance
- cited in PubMed and archived on PubMed Central
- yours — you keep the copyright

Submit your manuscript here:
http://www.biomedcentral.com/info/publishing_adv.asp

